PAPER • OPEN ACCESS

Abrasive water jet machining of CFRPs: single response optimization using taguchi method optimization

To cite this article: I I Edriys *et al* 2020 *IOP Conf. Ser.: Mater. Sci. Eng.* **973** 012029

IOP Conf. Series: Materials Science and Engineering **973** (2020) 012029 doi:10.1088/1757-899X/973/1/012029

Abrasive water jet machining of CFRPs: single response optimization using taguchi method optimization

I I Edriys[1], M Fattouh[2] and R Masoud[2]

[1]Kaha for chemical industries (270 army factor), Egypt
[2]Faculty of Engineering, Minufiya University, Shebin El Kom, Egypt
E-mail: Islam_edriys@yahoo.com

Abstract. Taguchi method was applied to assess and optimize machining parameters and their effect on kerf characteristics during abrasive water jet machining (AWJM) of carbon fiber reinforced polymeric composites (CFRPCs). The main responses selected for these analyses are kerf width, kerf taper, metal removal rate, and surface roughness, the consistent machining parameters focussed for this study are abrasive flow rate, pressure, traverse rate, thickness of the workpiece and standoff distance, each parameter has three levels. Twenty-seven experiments were conducted on a typical CFRP composite workpiece materials based on Taguchi L27 design. The response curves and response tables were used to assess the data obtained to control the major significant process factors statistically affecting the kerf characteristics. The optimal settings of process parameters for each response are set up. From the analysis, it was detected that the percentage contribution of the control factors affecting the kerf width is standoff distance, workpiece thickness, abrasive flow rate, traverse rate, and pressure correspondingly. The results exposed that the thickness, feed rate, and standoff distance were the most significant factors affecting the kerf taper, metal removal rate, and surface roughness respectively.

Introduction

Abrasive water jet machining (AWJM) is one of the most newly developed non-traditional cutting processes. It uses a fine jet of ultrahigh-pressure water and abrasive slurry to cut the board material by means of corroding. AWJ cutting is being progressively used to machine a wide-ranging of metals and non-metals, mainly ‘difficult-to-cut’ materials such as ceramics, marble, and fiber-reinforced polymeric composites, due to its various different advantages over other technologies such as no thermal distortion, high machining adaptability, ability to contour and small cutting force [1-2]. Since the introduction of the AWJ cutting technology for commercial use, a large amount of researches and progress has been made to discover its applications and related science [4-24]. However, this technology is still below progress and there are many features of the technology that persist to be fully understood [8]. The work presented in this paper describes experimental work that has been undertaken with the objective of improving the current absence of understanding in the AWJM of CFRP composites. The experimental results can be used to provide approvals for the selection of cutting parameters for AWJM applications. Definitely, the objective of the research described in this study is as follows: To achieve a detailed experimental study of the kerf characteristics when AWJM of CFRPCs to gain a complete understanding of the effects of several major process variables and to give optimum cut quality using Taguchi method.

IOP Conf. Series: Materials Science and Engineering **973** (2020) 012029 doi:10.1088/1757-899X/973/1/012029

Experimentation
The experimental work was accompanied on abrasive water jet cutting machine in which the tests were made is an OMAX 5555 jet machining center (figure 1). This model cuts multifarious flat parts out of most materials directly from a CAD drawing or DXF file. It includes a completely sealed and safe ball screw drive system, providing strength and dependability while offering high correctness. mixing tube of 0.762mm in diameter and 76.2mm in length were used to produce the AWJ. Garnet abrasives of 80 mesh (0.18 mm average diameter and 4.1 g/cm3 density) were applied. The CFRP composite material specimens used in this study were fabricated by stacking prepare, which is composed of one-way carbon fiber and epoxy resin bidirectional (0–90) and specimens were stacked to a total of 12, 24 and 36 plies respectively. The specimens were fabricated by compressing the material at a curing temperature of 125 °C using a heater located inside a cavity, with a curing time of 180 min and a forming pressure of 5 kg/cm2 as revealed in figure 2. The mechanical properties of the carbon-fiber prepares are publicized in Table 1. The specimen was 50x50 mm in vertical and horizontal direction figure 3.

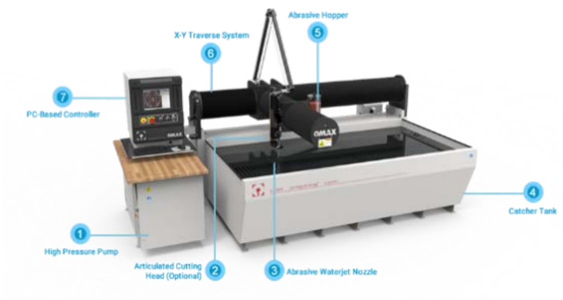

Figure 1. OMAX 5555 Jet Machining Centre

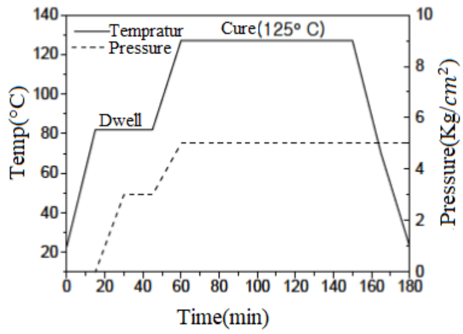

Figure 2. Stacking process for CFRPCs

The specimen was 50x50 mm in vertical and horizontal centring. Different workpiece geometries are planned to study the kerf characteristics in the straight cutting and profile cutting or contouring as presented in figure 3. The first geometry design is a straight cutting (kerf) as illustrated by figure 3. This design allows to measure the surface roughness on the depth of cut and to measure the distance between each cut side (kerf width) in the upper and lowest positions while providing the capability to picture the angle formed (kerf taper angle). MRR can be calculated. The second geometries design are square opining, hole opening, and external curving. The two holes characterized in the center of the plate were made for the resolve of holding it to the stand in the coordinate machine. In this paper, the experimental study is restricted to straight cutting under a range of AWJ process parameters.

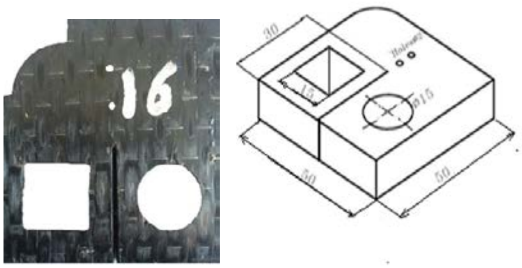

Figure 3. Geometry of the Workpiece.

Table 1. Mechanical properties of the Carbon-Fibre Sample

Properties	Value
Tensile strength (MPa)	5490
Tensile modulus (MPa)	294
Elongation (%)	1.9
Density (g/cm^3)	1.81

IOP Conf. Series: Materials Science and Engineering **973** (2020) 012029 doi:10.1088/1757-899X/973/1/012029

1.1. Experimental Design Methodology
A Taguchi orthogonal array is used in this investigation as an experimental plan. For ease and avoiding lengthy statement, the concept of Taguchi was offered and employed in Ross [3]. Table 2 illustrations the cutting parameters and their levels reflected for the experimentation on this paper. The parameters and levels were selected agreeing to the review of some papers [18-23] that has been recognized on AWJM on CFRPCs. Rendering to the Taguchi method, an L27 orthogonal array was working for the experimentation. Based on this, a total number of 27 experiments were done, each having a unlike combination of cutting parameters as shown in table 3. The responses were noted for each experimental run.

Table 2. Control factors (AWJM Parameters) and their levels.

Parameters	**symbol**	**Level**		
		1	**2**	**3**
Material Thickness (mm)	T	4	8	12
Water Pressure (MPa)	P	100	200	300
Traverse speed (mm/s)	V	1	3	5
Abrasive flow rate (g/min)	AFR	100	200	300
Standoff distance (mm)	SOD	2	4	6

Table 3. Orthogonal array.

Exp. No.	**T**	**P**	**V**	**A.F.R**	**S.O.D**	**Exp. No**	**T**	**P**	**V**	**A.F.R**	**S.O.D**
1	4	100	1	100	2	15	8	200	5	200	6
2	4	100	3	200	4	16	8	300	1	100	4
3	4	100	5	300	6	17	8	300	3	200	6
4	4	200	1	200	4	18	8	300	5	300	2
5	4	200	3	300	6	19	12	100	1	300	4
6	4	200	5	100	2	20	12	100	3	100	6
7	4	300	1	300	6	21	12	100	5	200	2
8	4	300	3	100	2	22	12	200	1	100	6
9	4	300	5	200	4	23	12	200	3	200	2
10	8	100	1	200	6	24	12	200	5	300	4
11	8	100	3	300	2	25	12	300	1	200	2
12	8	100	5	100	4	26	12	300	3	300	4
13	8	200	1	300	2	27	12	300	5	100	6
14	8	200	3	100	4						

1.2. Data Acquisition of Kerf Characteristics
Kerf width: A Portable 600x 3.6 MP digital microscope was used to measure the kerf width in upper and bottom positions. The measurements are occupied in three points: near to the upper edge, in the middle, near to lower edge of the Kerf and the usual value of measurements was used and preserved as the result of a single experiment for analysis (Figure 4).
Kerf taper: It was expected that in AWJ cutting the two kerf walls might not be regular due to the jet tailback effect. Figure 5. displays the kerf geometry.
The kerf taper can be acquired by measuring the upper and bottom kerf width and changing to taper kerf trend by the following relation:

$$\text{Kerf Taper Angle} \quad \theta = \tan^{-1}(W_t - W_b)/2T \qquad (1)$$

Where, W_t , W_b , T are the upper kerf width, bottom kerf width, and workpiece thickness correspondingly.
Metal Removal Rate (MRR): MRR for each experiment was calculated using the next formula:

$$MRR = 0.5\,(W_t + W_b).T.V \qquad (2)$$

Where V is cutting speed and unit for MRR is mm^3/sec.

Figure 4. Schematic Illustration of kerf image.

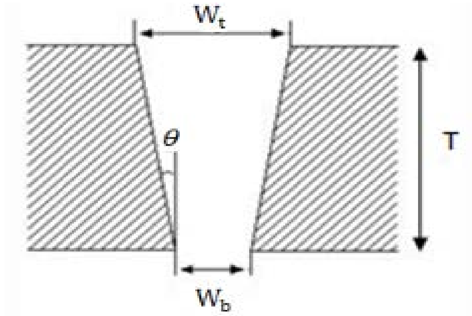

Figure 5. Schematic Illustration of Kerf Geometry.

Surface Roughness (R_a): The surface texture parameter for the Kerf throughout this investigated was the arithmetic mean roughness (R_a).
The measurements were taken at the direction of the cut in three areas: near to the upper edge, in the middle, near to lower edge in the center of the Kerf and the average value of measurements was used and treated as the result of a single experiment for analysis, figure 6. Figure 7 illustrations the kerf image.

The results of the four cut quality characteristics of kerf specifically, upper and bottom kerf width, taper angle, MRR and Ra for each of 27 trials are listed in Table 4. conferring to the performed experiment design.

Table 4. Results of experimental plan.

Exp. No.	Kerf (mm)		Taper Angle θ	MMR (mm^3/s)	SR (μm) Ra	Exp. No.	Kerf (mm)		Taper Angle θ	MMR (mm^3/s)	SR (μm)
	W_t	Wb					W_t	Wb			Ra
1	1.04	0.32	5.14	2.72	3.58	15	1.58	0.86	2.57	49.1	4.36
2	1.17	0.33	6.05	9.05	3	16	1.36	0.89	1.68	9.04	3.01
3	1.43	0.38	7.47	18.1	3.96	17	1.55	1.05	1.77	31.26	3.26
4	1.48	0.97	3.64	4.9	2.77	18	1.16	0.71	1.61	37.73	3.74
5	1.62	1.01	4.34	15.82	4.35	19	1.76	1.16	1.42	17.53	3.51
6	1.05	0.60	3.20	16.62	2.86	20	1.61	1.01	1.45	47.29	4.36
7	1.77	1.07	4.98	5.69	2.86	21	1.23	0.88	0.82	63.67	3.58
8	1.21	0.83	2.75	12.3	2.87	22	1.71	1.29	0.99	18.06	4.07
9	1.30	0.86	3.11	21.65	3.72	23	1.39	0.94	1.07	42.21	4.01
10	1.56	1	2.00	10.24	4.74	24	1.49	1.02	1.10	75.45	4.63
11	1.22	0.56	2.35	21.34	4.10	25	1.45	1.22	0.55	16.06	3.37
12	1.14	0.31	2.98	29.1	5.09	26	1.54	1.17	0.87	48.82	3.66
13	1.50	0.93	2.05	9.77	2.70	27	1.51	0.87	1.52	71.55	4.13
14	1.19	0.86	1.18	24.78	4.41						

IOP Conf. Series: Materials Science and Engineering **973** (2020) 012029 doi:10.1088/1757-899X/973/1/012029

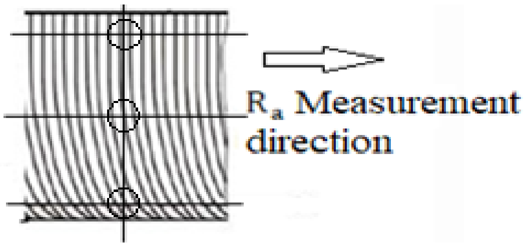

Figure 6. The Direction of Ra Measurement

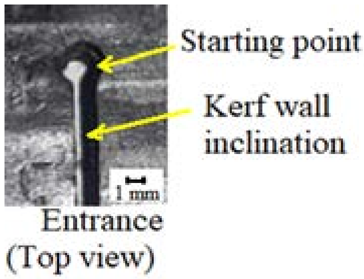

Figure 7. Image of Kerf Geometry

3. Result and Discussion

1.3. Effect of Process Variables on Kerf Top Width (W_t)

The average values of W_t for each parameter at levels 1, 2, and 3 for the raw data are schemed in figure 8. It shows that the W_t increases with the increase of T, AFR, and SOD where the standoff distance adopts the area of cutting which increases or decreases the impact area (whereas deviation of jet takes place with increase in stand-off distance), besides this, the effect of stray abrasive particles is prominent with high standoff distance with the rise of abrasive mass flow rate, cutting ability of jet that rises kerf top width and damage the surface. During increasing the abrasive particles (AFR), they own more energy to cut the material and they constantly lose the energy during decreasing its quantity. By the fact of increasing T, the time of piercing rise causes wider top kerf. Also, W_t decreases with increase in V due to less abrasive impingement at high traverse rate and results in less overlying of machining action, which reduces the kerf top width whereas the effect of water pressure is not important on W_t . It is also obvious that W_t is minimum at first level of SOD and maximum at third level of SOD.

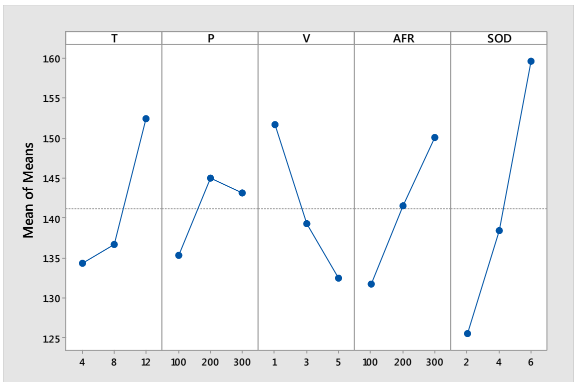

Figure 8. Effects of Process Parameters on W_t (Raw Data).

The response table 5 shows the average of W_t (S/N data) and its proportion contribution. The table contains ranks based on delta statistics, which equate the relative magnitude of effects. The delta statistic is the highest minus the deepest average for each factor. Minitab allocates ranks based on delta values; rank 1 to the highest delta value, rank 2 to the second-highest, and thus on. The ranks designate the relative importance of each factor to the response. The ranks and the delta values show that SOD has the highest effect on W_t and is tailed by T, AFR, V, and P in that order. From the analysis, it was saw that the percentage contribution of the control factors affecting the W_t is SOD (33.96%), T (18.81 %), AFR (18.78%), V (18.35%), and P (10.08%) one-to-one. As W_t is the "lower the better" type quality characteristic, it can be seen from figure 7 that the first level of T, first level of P, third level of V, first level of AFR, and first level of SOD offer minimum value of W_t. The S/N data analysis (Table 5) also advises the same levels of the variables (T = 4 mm, P =100 MPa, V= 5 mm/sec, AFR = 100 g/min and SOD 2 mm) as the best levels for minimum W_t. Because this combination parameters are selected from the response table (table 5) conferring to Taguchi analysis, and this combination parameters are not found in the orthogonal array (table 3), the confirmation test analysis for W_t is processed. The result of confirmation test analysis is associated with the initial condition of setting parameters. It is clear from table 4, that experiment No.7 has the poorest W_t value (1.77 mm) compared to the other experiments. therefore, it can be decided that experiment No. 7 possesses initial setting parameters. Table 6 displays the comparative results of the near-optimum setting parameters (T= 4 mm, P=100 MPa, V= 5 mm/sec, AFR= 100 g/min and SOD = 2mm) and initial setting parameters (T = 4 mm, P = 300 MPa, V= 1 mm/sec, AFR = 300 g/min and SOD = 6 mm). For the single performance characteristic, the W_t is reduced from 1.77 mm to 1.03 mm. The forecast (calculated) of W_t using the optimal level setting parameters can be calculated from Minitab 17. The conforming improvement in W_t is 58 %.

Table 5. Response for Signal to noise ratios of kerf width.

Level	T	P	V	A.F.R	S.O.D
1	-2.434*	-2.505*	-3.521	-2.267*	-1.906*
2	-2.641	-3.140	-2.807	-2.976	-2.742
3	-3.618	-3.047	-2.365*	-3.450	-4.045
Delta	1.185	0.635	1.156	1.183	2.139
Rank	2	5	4	3	1
contribution	18.81%	10.08%	18.35%	18.78%	33.96%

Table 6. Results of confirmatory experiment of kerf width

Worst value (Exp. No.7 Table.4.5)	W_t= 1.772 mm
Near optimum combination	T=4 mm, P =100 MPa, V= 5 mm/sec, AFR = 100 g/min and SOD 2mm
Predicted value (TAGUCHI)	W_t = 0.948 mm
Experimental value	W_t = 1.03 mm
Improvement %	1.029/1.772 = 58%

Figure 9 displays that there is very weak interaction between the process parameters in affecting the W_t since the responses at different levels of process parameters for a given level of parameter value are nearly parallel. It can be realized from figure 10 that the data follow a roughly straight line in normal probability plot display that the data are normally scattered.

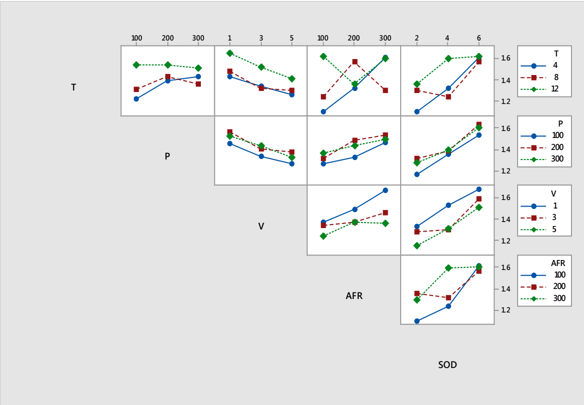

Figure 9. Effects of Process Parameters Interactions on W_t (Raw Data).

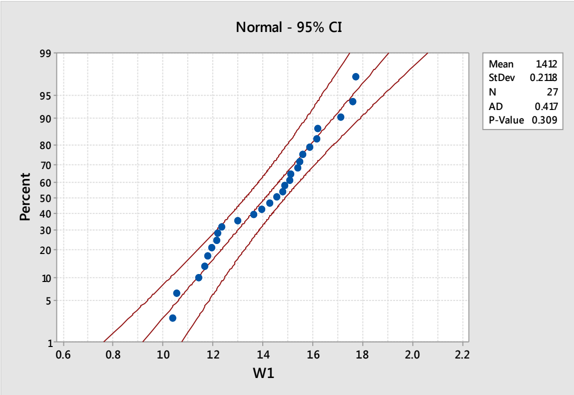

Figure 10. Normal Probability Plot for Kerf Top Width.

1.4. Effect of Process Variables on Kerf Taper (K_t)

Figure 11 illustrates that the K_t drops with the increase of T and P but increases with rise in AFR and SOD which the effect of V is frailly on K_t . During the jet penetrates into the material, the jet loses its kinetic energy when moving from upper surface to bottom surface, which reduced cutting ability constantly cases the kerf taper. The parameters similar jet pressure and feed rate decide the kinetic energy and the cutting time for the process and that control K_t. But the standoff distance agrees the area of cutting which rises or decreases the impact area cases high K_t at high level of SOD, with increase T the angle of cut by the jet penetration reduced cases little K_t.

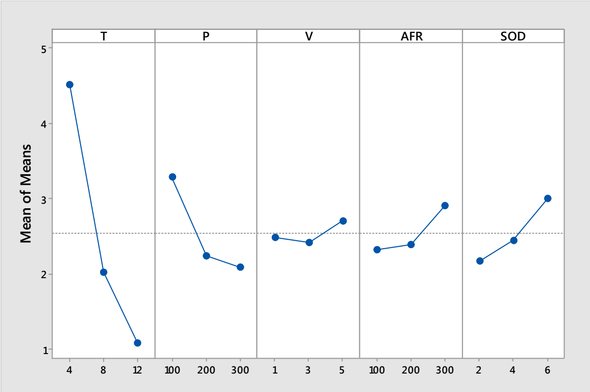

Figure 11. Effects of Process Parameters on $\mathbf{K_t}$ (Raw Data).

Table 7 displays the average of K_t (S/N data) and the optimal level setting parameters and its ratio contribution. Table 8 shows the forecast (calculated) value of K_t and the conforming improvement.

Table 7. Response for signal to noise ratios of kerf taper.

Level	T	P	V	A.F.R	S.O.D
1	-12.6725	-8.3357	-6.010	-6.1594	-4.98*
2	-5.8401	-5.7167	-5.975*	-5.5393 *	-6.1183
3	-0.3958*	-4.8559*	-6.922	-7.2097	-7.8039
Delta	12.2767	3.4798	0.947	1.6704	2.8178
Rank	1	2	5	4	3
contribution	57.93%	16.42%	4.4%	7.88%	13.29%

Table 8. Results of confirmatory experiment of kerf taper

Worst value (Exp. No.3 Table.4)	K_t = 7.477°
Near optimum combination	T=12mm, P =300MPa, V= 3mm/sec, AFR = 200 g/min and SOD 2 mm
Predicted value (TAGUCHI)	K_t=0.01°
Experimental value	K_t= 0.803°
Improvement %	0.803563/7.477 = 10.73%

Figure 12 displays that there is very frail interaction between the process parameters in touching the Kt since the responses at different levels of process parameters for a given level of parameter value are virtually parallel. It can be understood from figure 13 that the data follow a roughly straight line in normal probability plot indicates that the data are normally scattered.

IOP Conf. Series: Materials Science and Engineering **973** (2020) 012029 doi:10.1088/1757-899X/973/1/012029

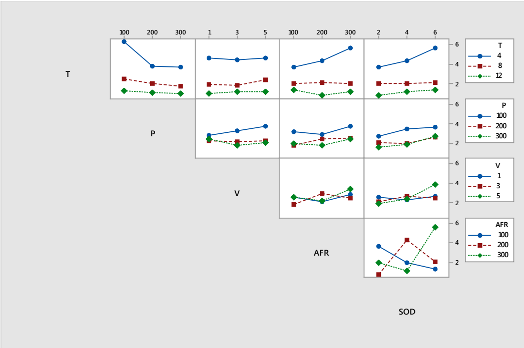

Figure 12. Effects of Process Parameters Interactions on K_t (Raw Data).

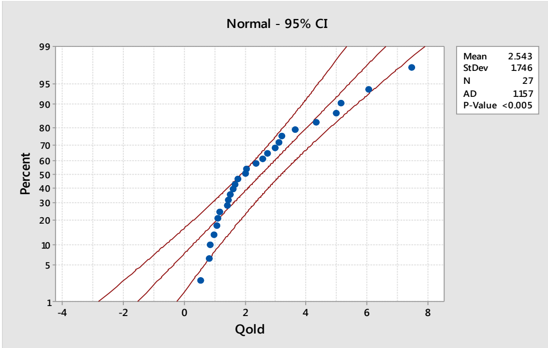

Figure 13. Normal probability Plot for Kerf Taper.

1.5. Effect of Process Variables on Metal Removal Rate (MRR)

Figure 14 displays that the MRR rises with the rise of T and V, and the effects of both P, AFR and SOD is frailly on MRR. By the fact of growing kinetic energy due to an increase in V, T, and P that give higher MRR which rises in feed rate and pressure the abrasive particle becomes less time to cut the higher material thickness and new particles arrive in cutting region. Also, aids to remove more volume of material. Also, the effect of SOD is frail because the deviation in jet and low kinetic energy of the abrasive particles due to more distance between the jet and the workpiece beside the sharp cutting of the material is not possible, the cutting ability reduced during traveling owing to distance travelled that reduces its capability of material removal but SOD increase the cutting region and remove higher MRR.

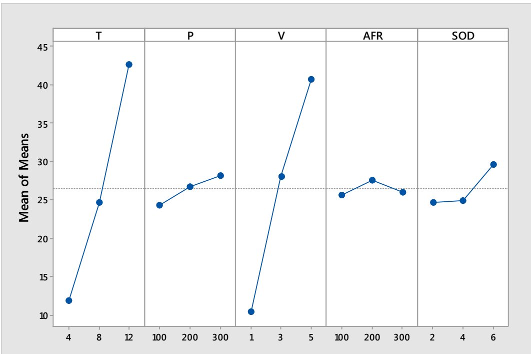

Figure14. Effects of process parameters on MRR (Raw Data).

Table 9 displays the average of MRR (S/N data) and the optimal setting parameters and its percentage contribution. Table 10 shows the forecast (calculated) value of MRR and the corresponding progress. The near optimum setting parameters (T = 12 mm, P =300 MPa , V= 5 mm/sec , AFR = 300 g/min and SOD = 6 mm).

Table 9. Response for Signal to noise ratios of MRR.

Level	T	P	V	A.F.R	S.O.D
1	19.87	24.83	18.98	25.21	25.06
2	26.46	26.54	27.67	26.25	25.79
3	31.63*	26.57 *	31.29*	26.49 *	27.10*
Delta	11.76	1.74	12.31	1.27	2.04
Rank	2	4	1	5	3
contribution	40.38	5.97%	42.27%	4.36%	7.00%

Table 10. Results of confirmatory experiment of MRR.

Worst value (Exp. No.1 Table4)	MRR = 2.72 mm
Near optimum combination	P =300 MPa, V= 5 mm/sec, AFR = 300g/min and SOD = 6 mm
Predicted value (TAGUCHI)	76.32 mm^3/sec
Experimental value	MRR= 75.69 mm^3/sec
Improvement %	2.72/75.69 = 3.59%

Figure 15 displays that there is very frail interaction between the process parameters in affecting the MRR since the responses at different levels of process parameters for a given level of parameter value are nearly parallel. It can be understood from figure 16 that the data follow an approximately traditional line in normal probability plot designates that the data are normally distributed.

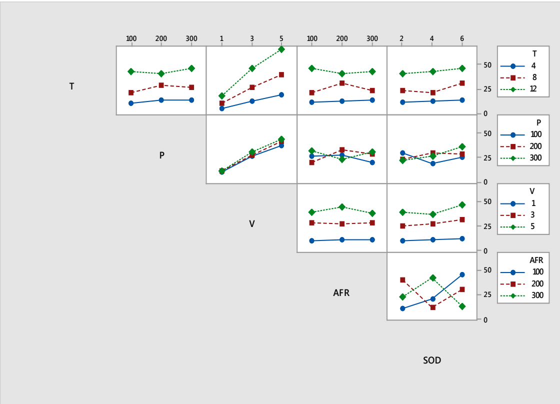

Figure 15. Effects of Process Parameters Interactions on MRR

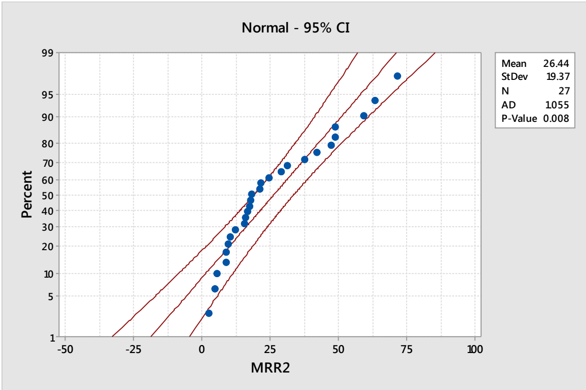

Figure 16. Normal Probability Plot for MRR

1.6. Effect of Process Variables on Surface Roughness (R_a)

Figure 17 displays that the R_a rises with the increase of T, V, and SOD, and decreases with an increase in P where lower pressure deteriorated the finish on the cut surface by creating lays and flaws with observed strong scratches and grooves, resulting in a poor finish. Also, with increasing the area of cut surface by increasing T there is more lays and flaws and the surface waviness produced a large difference between the peak and valley from the mean line, resulting in a poor finish. The excessive abrasives penetrate into the layers of material which result in abrasive embedment. Abrasive embedment is mainly observed at high AFR and low SOD. At low SOD, abrasives cannot accelerate with high-speed water jet which causes abrasives to impinge on material with low kinetic energy. These abrasives penetrate into the layers and machined surface cases rough surface. There are small effects of AFR. which the jet lag at higher V resulted because of insufficient time for cutting the CFRP. Thus, the fibers that poked out from the cut surface got forced up with the stylus probe during measurement, increasing the roughness. With the overlapping of machining action and also reduced number of abrasive particles to impinge on surface. Also, at low pressure, the surface waviness produced a large difference between the peak and valley from the mean line, resulting in a poor finish. However, the increased energy at high pressure improved the cutting efficiency and produced a smooth surface. Figure 18 displays the defects and damage in the cut surface.

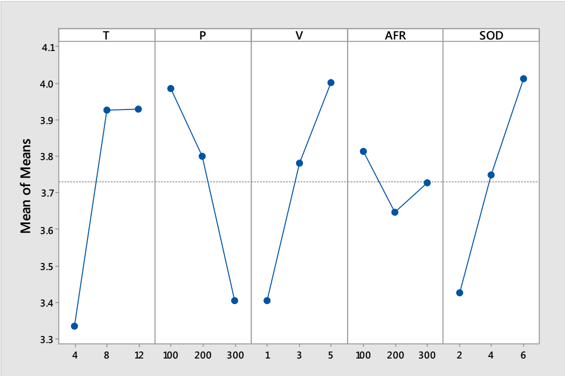

Figure 17. Effects of Process Parameters on R_a (Raw Data).

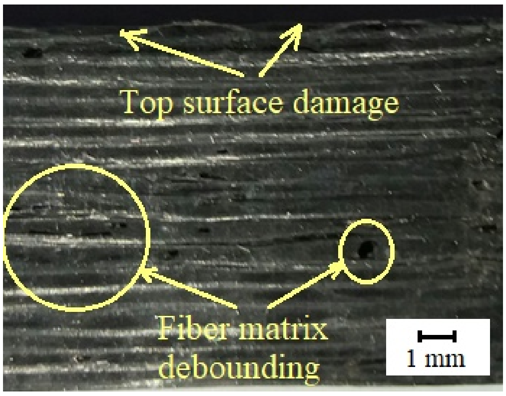

Figure 18. Stacking process for CFRPCs.

Table 11 displays the average of R_a (S/N data) and the optimal setting parameters and their percentage contribution. Which table 12 shows the predicted (calculated) value of R_a and the conforming improvement.

Table 11. Response for signal to noise ratios of surface roughness.

Level	T	P	V	A.F.R	S.O.D
1	-10.35*	-11.91	-10.50*	-11.46	-10.61*
2	-11.71	-11.41	-11.45	-11.12*	-11.31
3	-11.84	-10.58*	-11.94	-11.31	-11.98
Delta	1.49	1.33	1.44	0.34	1.37
Rank	1	4	2	5	3
contribution	24.95%	22.27%	24.12%	5.69%	22.94%

Table 12. Results of confirmatory experiment of surface roughness.

Worst value (Exp. No.12 Table.4.5)	R_a = 5.09 µm
Near optimum combination	T=4 mm, P =300 MPa, V= 1mm/sec, AFR = 200 g/min and SOD 2 mm
Predicted value (TAGUCHI)	R_a = 2.301 µm
Experimental value	R_a = 2.498 µm
Improvement %	2.698 /5.09 = 53.96%

Figure 19 shows that there is very weak interaction between the process parameters in affecting the R_a since the responses at different levels of process parameters for a given level of parameter value are greatest parallel. It can be seen from figure 20 that the data follow an approximately traditional line in normal probability plot indicates that the data are normally scattered.

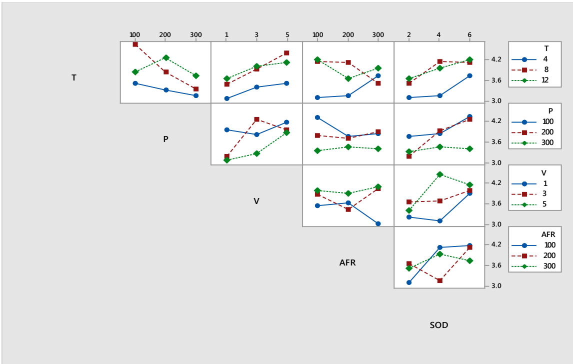

Figure 19. Effects of Process Parameters Interactions on Surface Roughness

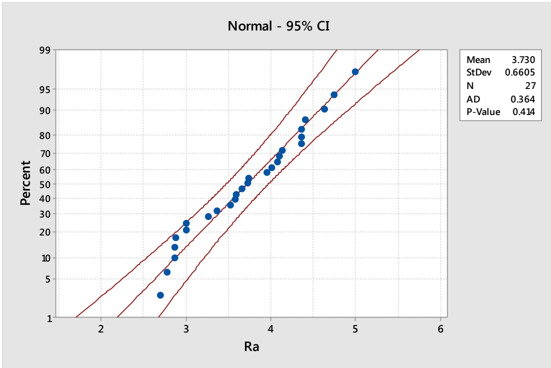

Figure 20. Normal Probability Plot for Surface Roughness

Conclusions

In cutting CFRPs using AWJM, numerous process parameters have effect on the performance measures. The effect of process variables on the characteristics of straight cutting was discussed. The optimal process parameters are found for various performance measures using the Taguchi design of experiment methodology. (single response optimization). The following assumptions can be drawn from the results of the present work:

1) SOD has the utmost effect on W_t and is trailed by T, AFR, V, and P in that order. From the analysis, it was detected that the percentage contribution of the control factors affecting the W_t is SOD (33.96%), T (18.81 %), AFR (18.78%), V (18.35%), and P (10.08%) respectively.
2) W_t rises with the increase of T, AFR, and SOD, also, W_t decreases with rise in V.
3) K_t decreases with the rise of T and P, also, Kt increases with rise in AFR and SOD. V has a very frail influence.
4) There is a very frail interaction by the process parameters on affecting the $\mathbf{K_t}$
5) MRR increases with the increase of T and V, and the outcome of P, AFR and SOD are frailly on MRR.
6) From the analysis, it was noticed that the percentage contribution of the control factors affecting the MRR is V (42.27%), T (40.38 %), SOD (7.00%), P (5.97%), and AFR (4.36%) respectively.
7) R_a rises with the increase of T, V, and SOD, and decreases with an increase in P.

References

[1] Luttervelt C A v 1989 On the selection of manufacturing method illustrated by an overview separation technique for sheet materials *Annals of the CIRP* **38**(2) pp 587-607.

[2] Ramulu M, and D Arola 1994 The influence of abrasive waterjet cutting conditions on the surface quality of graphite/epoxy laminates *International Journal of Machine Tools and Manufacture* **34** pp 295-313.

[3] Ross P J 1996 *Taguchi Technique for Quality Engineering second edition* (McGraw-Hill, NewYork).

[4] Arola D and M Ramulu 1996 A study of kerf characteristics in abrasive waterjet machining of graphite/epoxy composite *J. of engineering materials and technology* **118** pp 256-265.

[5] Hocheng H, Tasi H Y, Shiue J J and Wang B 1997 Feasibility study of Abrasive water jet milling of fiber-reinforced plastics *Journal of manufacturing science and engineering* **119** pp 133-142.

[6] Arola D and Ramulu M 1997 Material removal in abrasive waterjet machining of metals Surface integrity and Texture *Wear* **210** pp 50-58.

[7] Jun W 1999 A machinability study of polymer matrix composites using abrasive waterjet cutting technology *Journal of Materials Processing Technology* **94/1** pp 30-35.

[8] H Liu 2004 A study of the cutting performance in abrasive water jet contouring of alumina ceramics and associated jet dynamic characteristics (Queensland university of technology Ph

D Dissertation).
[9] Azmir M A and Ahsan A K 2009 A study of abrasive water jet machining process on glass/epoxy composite laminate *Journal of Materials Processing Technology* **209** pp 6168–6173.
[10] Tauseef U S, Mukul S and Pankaj B T 2009 Comparative investigation of abrasive water cut kerf quality characteristics for aramid, glass, and carbon fiber-reinforced composites used in transport aircraft applications *American WJTA Conference and Expo* August 18-20 (Houston, Texas).
[11] Ramulu M, I Hwang and V Isvilanonda 2009 Quality Issues Associated with Abrasive Water jet Cutting and Drilling of Advanced Composites *American WJTA Conference and Expo* (Hou., TX).
[12] Shanmugam D K and Masood S H 2009 An investigation on kerf characteristics in abrasive water jet cutting of layered composites *Journal of Materials Processing Technology* **209** pp 3887–3893.
[13] Alberta A, Suáreza A, Artazaa T, Escobar G A, Ridgwayb K 2013 Composite Cutting with Abrasive Water Jet *the Manufacturing Engineering Society International Conference* (MESIC) pp 421-429.
[14] Badgujar P P and Rathi M G 2014 Abrasive waterjet machining-A state of Art IOSR *Journal of Mechanical and Civil Engineering* **11** Issue 3 pp 59-64.
[15] Prasad D U, M D Gayakwad, N G Patil, R S Pawade, D G Thakur and P K Brahmankar 2015 Experimental Investigations into Abrasive Waterjet Machining of Carbon Fiber Reinforced Plastic *Journal of Composites* vol 2015 Article ID 971596 pp 9.
[16] Jignesh K P and Abdulhafiz A S 2015 The Influence of Abrasive Water Jet Machining Parameters on Various Response-A review *Int. J. Mech. Eng. & Rob. Res* **4** No 1 pp 383-403.
[17] Vishal S, R S J and Sakshi G 2015 A Review paper on most significant and subsignificant parameters of abrasive water jet machining *International Journal of Advance Research in Science and Engineering* **4** Iss 1 pp 249-256.
[18] Neelambari K S, Mangesh Y K and Vilas B S 2016 A Review on Parameters Optimization in Abrasive Water Jet Cutting *International Journal of Innovative and Emerging Research in Engineering* **3** Iss 2 pp 11-14.
[19] Rajyalakshmi M and P Suresh B 2016 Abrasive Water Jet Machining - A Review on Current Development *International Jour of Science Techn. & Engineering* **2**, Iss 12 pp 428-434.
[20] Rushabh B J, Dr A A Shaikh and Brijesh K G 2016 A Review on Abrasive Water Jet Machining On Different Material *International Journal of Engineering Development and Research* **4** Iss 2 pp 860-866.
[21] Ajit D, Shailendra K and R V Karmakar 2016 Abrasive Water Jet Machining of Carbon Epoxy Composite *Defence Science Journal* **66** pp 522-528.
[22] Thirumalai S K, Tae J K and M Uthayakumar 2017 Prediction of surface roughness in abrasive water jet machining of CFRP composites using regression analysis *Journal of Alloys and Compounds* **724** Iss 1 pp 249-256.
[23] Kumaran S T, Tae J K, R Kurniawan, C Li and M Uthayakumar 2017 ANFIS modeling of surface roughness in abrasive waterjet machining of carbon fiber reinforced plastics *Journal of Mechanical Science and Technology* **31**(8) pp 3949-3954.
[24] Irina W M M, Azwan I A, Lee C C and Ahmad F M 2017 Experimental study and empirical analyses of abrasive waterjet machining for hybrid carbon/glass fiber-reinforced composites for improved surface quality *The International Journal of Advanced Manufacturing Technology*.

Acknowledgments
Authors would like to thank Eng. Mohamed Daw director of Daw design Company at Cairo. Egypt, for providing the opportunity to accomplish the experimental work on OMAX 5555 Jet Machining Centre.